Human Cell (2020) 33:479–489
https://doi.org/10.1007/s13577-019-00315-8

RESEARCH ARTICLE

The miR-590-3p/VEGFA axis modulates secretion of VEGFA from adipose-derived stem cells, which acts as a paracrine regulator of human dermal microvascular endothelial cell angiogenesis

Yang Sun[1] · Xiang Xiong[1] · Xiancheng Wang[1]

Received: 4 July 2019 / Accepted: 13 December 2019 / Published online: 10 April 2020

Abstract

The paracrine secretion of angiogenic cytokines from adipose-derived stem cells (ADSCs) might promote endothelial cell angiogenesis, therefore promoting wound healing in injured tissues. Hypoxia is one of the common occurrence in injured tissues, during which angiogenesis is enhanced to improve the oxygen supply. In the present study, miR-590-3p, an anti-angiogenic miRNA, was predicted to target VEGFA, a key factor that can be transcriptionally upregulated by HIF1A during ADSC proliferation and tubule formation in response to hypoxic stimulation. Herein, we found that in response to hypoxic stimuli, HIF1A and VEGFA protein expressions were remarkably induced. In addition, ADSC viability was promoted. Incubation with conditioned medium from ADSCs stimulated by hypoxia significantly enhanced the angiogenic ability of human dermal microvascular endothelial cells (HDMECs), while the conditioned medium from VEGFA-silenced ADSCs significantly reversed the angiogenic ability of HDMECs. Regarding the molecular mechanism, it was verified that miR-590-3p binds to VEGFA; miR-590-3p inhibited VEGFA to affect the paracrine regulation by ADSCs, subsequently hindering the HDMEC angiogenesis. More importantly, the consequences of miR-590-3p-overexpressing conditioned medium on HDMEC angiogenesis were partially reversed by VEGFA-overexpressing conditioned medium. In conclusion, miR-590-3-5p/VEGFA axis modulates the paracrine secretion of VEGFA by ADSCs to affect the angiogenesis of HDMECs.

Keywords Adipose-derived stem cells (ADSCs) · Human dermal microvascular endothelial cells (HDMECs) · miR-590-3-5p · VEGFA

Introduction

Implants, which can be made from autogenous tissues or synthetic materials, are used to replace tissues and organs damaged or injured after trauma, cancer resection or congenital disease. For both kinds of implants, the survival of large tissue replacements of damaged organs depends on the formation of sufficient blood supply [1, 2]. Angiogenesis represents the formation of a new blood vessel network. This complicated and structural process is involved in the proliferation and migration of endothelial cells and the development of new blood vessels from preexisting ones [1, 2]. Therefore, effective and prompt revascularization can be the key to paracrine secretion of transplanted tissue, thus performing the desired function recovery [3, 4].

The application of mesenchymal stem cells (MSCs) in implants has been regarded as an effective approach for promoting the formation of blood vessels of tissue-engineered structures. Mesenchymal stem cells have been shown to promote angiogenesis in ischemic conditions by secreting growth factors, including VEGF [5]. A particular population of adult mesenchymal stem cells that has been extensively used to promote the formation of blood vessels of tissue-engineered structures is adipose-derived stem cells (ADSCs) [6], which can secrete various angiogenic cytokines to stimulate angiogenesis [7, 8]. Hypoxic stimulation can induce paracrine secretion of multiple cytokines from MSCs [9, 10]; after the migration of ADSCs to hypoxic regions, many therapeutic paracrine cytokines are produced by ADSCs to heal injured tissues [11]. A wide range of ADSC-secreted

Yang Sun and Xiang Xiong contributed equally to this study.

✉ Xiancheng Wang
wangxiancheng64@csu.edu.cn

[1] Department of Plastic Surgery and Burns Surgery, The Second Xiangya Hospital, Central South University, Hunan 410011, China

growth factors, such as autologous-inducing factors in tissue repair, has been observed in recent years, including VEGF, insulin-like growth factor (IGF), platelet-derived growth factor (PDGF), transforming growth factor-beta (TGF-β), and fibroblast growth factor (FGF) [12–14]. The levels of VEGF and its receptors (VEGF-R2, VEGF-R3), epidermal growth factor (EGF), and FGF were remarkably higher within the exosomes from human ADSCs under hypoxia stress than they were in homeostatic exosomes [15]. Hypoxia activates hypoxia-inducible factor (HIF-1α) which modulates angiogenic gene transcription, including VEGF and VEGFRs, to promote angiogenesis. Interestingly, in preliminary experiments, we have revealed that out of IGF-1, VEGFA, IL-10, IL-6, and IL-1β, the concentration of VEGFA was the most increased in ADSCs in response to hypoxic stimulation (Fig. 1c); thus, we speculate that hypoxic preconditioning of ADSCs might increase the levels and the paracrine of VEGFA and promote the angiogenesis of endothelial cells.

In addition to growth factors, another type of small RNA, namely, miRNAs which were once regarded as "genetic noise", might also be essential for the formation of blood vessels of endothelial cells through the posttranscriptional modulation of gene expression [16, 17]. LncRNA HIF1A-AS2 sponges miR-153-3p to promote HIF-1α upregulation,

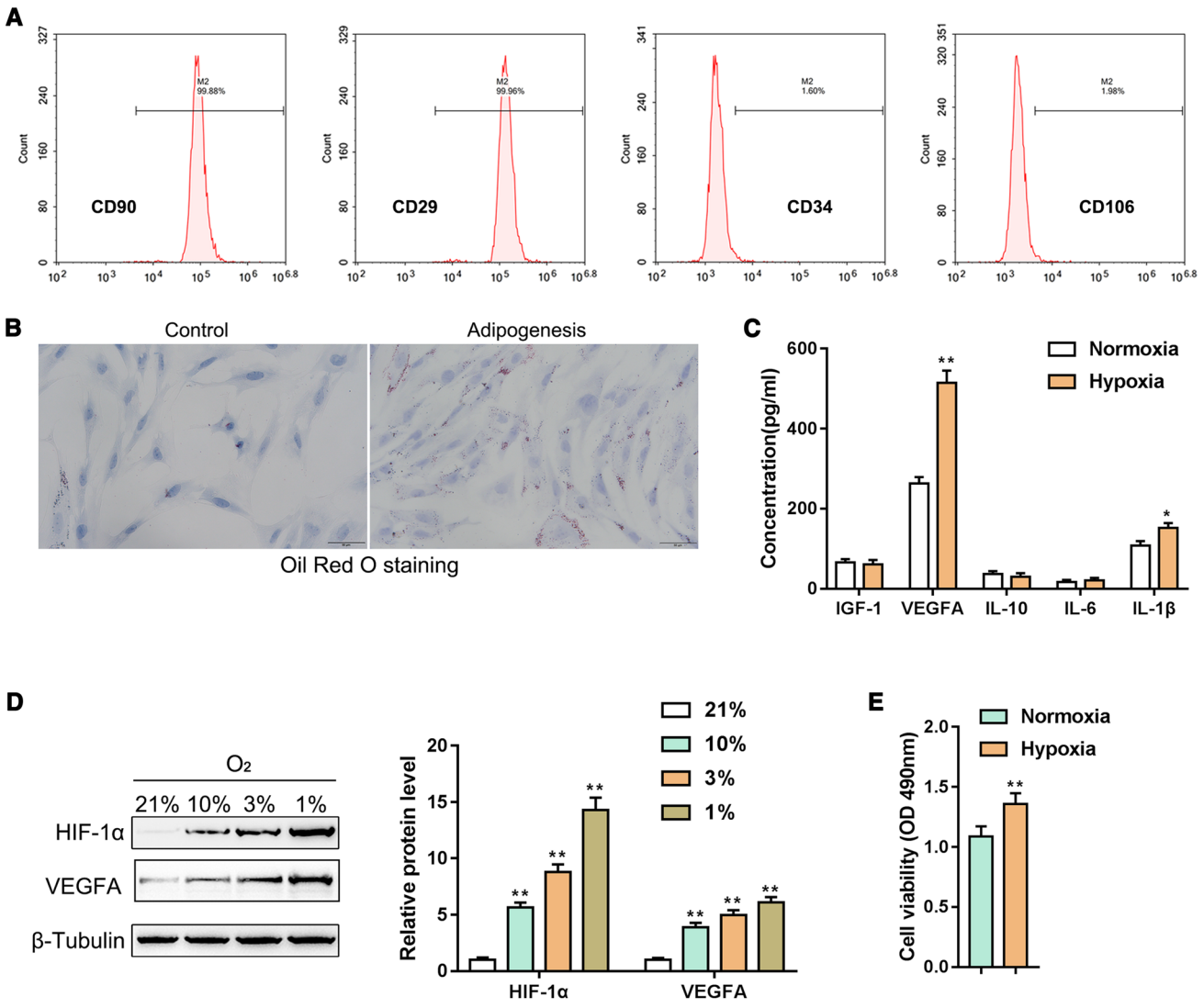

Fig. 1 Characterization of ADSCs and the responses of ADSCs to hypoxia stimulation. **a** The immunophenotype of ADSCs (CD90, CD29, CD45, and CD106) was determined by flow cytometry using antibodies against CD90, CD29, CD45, and CD106, $N=3$. **b** The adipogenic differentiation of ADSCs was examined by oil red O staining, $N=3$. **c** ADSCs were exposed to 1% and 21% O_2 and then were examined for the secretion of IGF-1, VEGFA, IL-10, IL-6, and IL-1β. VEGFA was selected for further experiments, $N=5$. **d** ADSCs were exposed to 1%, 3%, 10%, and 21% O_2 for 12 h and then maintained in normoxic conditions for 24 h; the protein levels of HIF-1A and VEGFA were determined by immunoblotting, $N=5$. **e** ADSCs were exposed to 1% O_2 for 12 h and then maintained in normoxic conditions for 24 h. Cell viability was determined by MTT assay, $N=5$. $^*P<0.05$, $^{**}P<0.01$

thus improving the formation of blood vessels within HUVECs during hypoxia [18]. Inhibition of miR-590-3p induced by YKL-40, a proinflammatory protein, promotes IL-18 expression and endothelial progenitor cell angiogenesis [19]. miR-26a interacts with the BMP/SMAD1 signaling pathway in endothelial cells to modulate pathological and physiological angiogenesis [20]. The upregulation of miR-29b induced by berberine contributes to ischemia-induced angiogenesis in mouse hearts [21]. In BMP4-stimulated human umbilical vein endothelial cells (HUVECs), miR-494 has been reported to be significantly downregulated; the overexpression of miR-494 hinders the angiogenic function of endothelial cells and miR-494 inhibition-enhanced angiogenesis [22]. miR-16 is an miRNA that is thought to target VEGF, and it is enriched in MSC-derived exosomes; miR-16 is partially responsible for the anti-angiogenesis effect of MSC-derived exosomes [23]. Exosomal miR-320 downregulates its target genes, including IGF-1, Hsp20, and Ets2, in the cardiac endothelial cells of recipient mice, and miR-320 overexpression hinders mouse cardiac endothelial cell migration and tubule formation [24]. Thus, we hypothesize that miRNAs might be involved in paracrine VEGFA production by ADSCs and the subsequent angiogenesis of endothelial cells.

Herein, we first determined the properties and the differentiation potential of ADSCs and then we examined the mRNA expression and protein levels of HIF1A and VEGFA in ADSCs, as well as the cell viability of ADSCs in hypoxic conditions. The specific effects of VEGFA silencing on the DNA synthesis ability, cell migratory capacity, and vascularization of ADSCs were examined in hypoxic conditions. Next, the putative binding between miR-590-3p and VEGFA and the relationships between miR-590-3p overexpression in ADSCs and VEGFA expression and HDMEC angiogenesis were investigated under normoxic and hypoxic conditions. Afterward, the dynamic effects of miR-590-3p and VEGFA overexpression in ADSCs on HDMEC angiogenesis were evaluated in hypoxic conditions. These data have demonstrated that a miR-590-3p/VEGFA axis that could modulate VEGFA secretion by ADSCs, thereby affecting the angiogenesis of HDMECs.

Materials and methods

Cell culture and hypoxia stimulation

Primary human ADSCs (ADSCs) were purchased from ATCC (PCS-500-011™, Manassas, VA). Cells were cultured in Dulbecco's modified Eagle medium (DMEM, Gibco, CA, USA) with 10% FBS and 1% antibiotics (named proliferation medium, PM) for proliferating. The immunophenotype of ADSCs, including CD90, CD29, CD34, and CD106 were analyzed by flow cytometry (BD, San Jose, CA, USA). The verification of adipogenic differentiation was performed by oil red O staining as described previously [25]. Passage 2–4 ADSCs were used.

HDMECs were obtained from Sciencell (San Diego, CA, USA) and were cultured in an endothelial cell medium (Sciencell) supplemented with 5% FBS, 1% endothelial cell growth supplement, and 1% penicillin/streptomycin solution. Cells were cultured in 5% CO_2 at 37 °C until they reached 70–80% confluence.

For construction of the hypoxia-induced injury model, ADSCs were exposed to 1%, 3%, 10%, and 21% O_2 for 12 h, and then were introduced to normoxia for an additional 24 h.

Cell differentiation

Proliferation medium (PM) supplemented with 50 nM insulin, 100 nM dexamethasone, 0.5 mM 3-isobutyl-1-methylxanthine, and 200 μM indomethacin (differentiation-inducing medium, DM) was used for the induction of adipogenic differentiation.

Cell transfection

VEGFA knockdown was achieved by transfection with si-VEGFA (at a final concentration of 100 nM GeneChem, Guangzhou, China). VEGFA overexpression was achieved by transfection with a pcDNA-VEGFA expression vector (at a final concentration of 1 μg/ml, GeneChem). The expression of miR-590-3p was achieved by transfection with miR-590-3p mimics or an inhibitor (at a final concentration of 50 nM, Genepharma, Shanghai, China) with the help of Lipofectamine 2000 (Invitrogen). The sequences are shown in Table 1.

Protein level determination by immunoblotting

Cells were lysed for protein extraction, and the protein was separated using an SDS-PAGE mini-gel. Protein samples were then transferred to a PVDF membrane and probed at 4 °C overnight with the following primary antibodies obtained from Abcam (Cambridge, MA, USA): anti-HIF1-α (ab82832), anti-VEGFA (ab1316), anti-β-Tubulin (ab6046). Then the membrane was incubated with HRP-conjugated secondary antibody. Afterward, an enhanced chemiluminescence detection kit (Beyotime, Biotechnology, China) was used to visualize the signals. The protein level of β-tubulin was employed for endogenous normalization when analyzing the gray intensity, which was done using ImageJ software (NIH, Bethesda, MD, USA).

Table 1 Primer sequence

Name	Forward	Reverse
Si-NC	UUC UCC GAA CGU GUC ACG UTT	ACG UGA CAC GUU CGG AGA ATT
Si-VEGFA 1	CGACAAAGAAAUACAGAUATT	UAUCUGUAUUUCUUUGUCGTT
Si-VEGFA 2	GGUUAAUAUUUAAUUUCAATT	UUGAAAUUAAAUAUUAACCTT
Si-VEGFA 3	GAGAAUUCUACAUACUAAATT	UUUAGUAUGUAGAAUUCUCTT
miR-NC	UUCUCCGAACGUGUCACGUTT	ACGUGACACGUUCGGAGAATT
MiR-590-3p mimics	UAAUUUUAUGUAUAAGCUAGU	UAGCUUAUACAUAAAAUUAUU
miR-590-3p inhibitor	ACUAGCUUAUACAUAAAAUUA	
Inhibitor-NC	CAGUACUUUUGUGUAGUACAA	
QPCR		
MiR-153-3p	RT: GTCGTATCCAGTGCGTGTCGTGGAGTCGGC AATTGCACTGGATACGACGATCAC F: GCCTTGCATAGTCACAAAA	R: CAGTGCGTGTCGTGGA
MiR-590-3p	RT: GTCGTATCCAGTGCGTGTCGTGGAGTCGGC AATTGCACTGGATACGACACTAGC F: GCCGGCCTAATTTTATGTATAA	R: CAGTGCGTGTCGTGGA
MiR-26a-5p	RT: GTCGTATCCAGTGCGTGTCGTGGAGTCGGC AATTGCACTGGATACGACAGCCTA F: GCCTTCAAGTAATCCAGGA	R: CAGTGCGTGTCGTGGA
MiR-29b	RT: GTCGTATCCAGTGCGTGTCGTGGAGTCGGC AATTGCACTGGATACGACCTAAGC GCCTGGTTTCACATGGTG	R: CAGTGCGTGTCGTGGA
MiR-494	RT: GTCGTATCCAGTGCGTGTCGTGGAGTCGGC AATTGCACTGGATACGACGAGGTT F: GCTGAAACATACACGGGA	R: CAGTGCGTGTCGTGGA
MiR-16	RT: GTCGTATCCAGTGCGTGTCGTGGAGTCGGC AATTGCACTGGATACGACCGCCAA F: GCCTAGCAGCACGTAAATA	R: CAGTGCGTGTCGTGGA
MiR-320	RT: GTCGTATCCAGTGCGTGTCGTGGAGTCGGC AATTGCACTGGATACGACTCGCCC F: GCAAAAGCTGGGTTGAGA	R: CAGTGCGTGTCGTGGA
U6	CTCGCTTCGGCAGCACATATACT	ACGCTTCACGAATTTGCGTGTC
VEGFA	AGGGCAGAATCATCACGAAGT	AGGGTCTCGATTGGATGGCA
β-Tubulin	GACTGTCTCCAGGGCTTCCA	GAGTAGGTTTCATCTGTGTTTTCCA
Plasmid construction		
Wt-VEGFA 3′UTR	CCGCTCGAGATCTTTTGCTCTCTCTTGCTCT	AAATATGCGGCCGCCTATTTTTTCTTGTTTTGTTTTTAC
Mut-VEGFA 3′UTR	GACAGTCAGATCGATATCTTGAACAGATATTTAATTTTGCTAACACT	GATATCGATCTGACTGTCACCGATCAGGGAGAG
VEGFA overexpression	AAATATGCGGCCGCCTGACGGACAGACAGACAGACACC	CCGCTCGAGTCACCGCCTCGGCTTGTC

Polymerase chain reaction (PCR)-based analyses

Total RNA was extracted, processed, and examined for the expression of target mRNAs and miRNAs following previously described methods [26]. mRNA and miRNA expression was detected by an SYBR green PCR Master Mix (Qiagen, Hilden, Germany) using β-tubulin (for mRNA examination) or RNU6B (for miRNA examination) as an endogenous control. The data were analyzed using a $2^{-\Delta\Delta CT}$ method. The primer sequences are shown in Table 1.

Luciferase reporter assay

To validate the predicted binding between miR-590-3p and the VEGFA 3′-UTR, we constructed wild- and mutant-type VEGFA 3′-UTR luciferase reporter vectors by cloning the wild-type VEGFA 3′-UTR downstream of the Renilla psiCHECK2 vector (Promega, Madison, WI, USA) or by mutating the predicted miR-590-3p binding site. 293T cells (ATCC, USA) were cotransfected with these vectors and miR-590-3p mimics or an miR-590-3p inhibitor. Luciferase

activity was determined using a Dual-Luciferase Reporter Assay System (Promega, Madison, WI, USA), and we used firefly luciferase activity for normalization.

Analysis of cytokines by ELISA

The culture medium was collected for ELISA using human IGF-1, VEGFA, IL-10, IL-6, and IL-β1 ELISA kits according to the manufacturer's instructions (Santa Cruz Biotechnology, Santa Cruz, CA, USA). The specific binding optical density was immediately assayed immediately at 450 nm with a spectrophotometer (Bio-Rad Laboratories).

DNA synthesis determined by EdU assay

EdU (5-ethynyl-2′-deoxyuridine) is a nucleoside analog of thymidine that is incorporated into DNA during active DNA synthesis. Incorporation of EdU into genomic DNA in the S-phase is detected based on a click reaction between the alkyne moiety of EdU and a fluorescent azide. DNA synthesis ability was detected by EdU assays using an EdU assay kit (RiboBio, Guangzhou, China) following a previously described method [27]. The cells containing newly synthesized DNA were labeled by green fluorescence. The nucleus was stained with DAPI. Representative images were taken under an IX71 fluorescence microscope (Olympus, Tokyo, Japan).

Cell migration determined by transwell assays

For the Transwell migration assays, HDMECs were seeded onto the upper chambers of transwell 24-well plates (Corning, Corning, NY, USA) at a density of 1×10^5 cells/well with 8 μm pore filters. The polycarbonate transwell filters without Matrigel on the upper chambers were used for migration analysis. A medium without serum was used to suspend the cells suspended in the upper chambers and a medium with serum was added to the bottom chambers for the migration analyses. After 12 h, the cells attached on the upper surface of the filter membranes were cleaned and the migrated cells on the membrane surface of the bottom chambers were fixed with 4% paraformaldehyde and then stained with 0.5% crystal violet (Sigma Aldrich, St. Louis, MO, USA). Observing the cells and capturing their images were performed under an optical microscope (Olympus CKX53, Tokyo, Japan).

ADSC effects on HDMEC tube formation under hypoxic conditions

The impacts of paracrine release from ADSCs (including VEGFA silenced, miR-590-3p overexpressed, and miR-590-3p and VEGFA co-overexpressed) on HDMEC angiogenesis were evaluated using BD Matrigel wells (BD Biosciences, Franklin Lakes, NJ, USA). HDMECs were seeded into 96-well microtiter plates coated with Matrigel (80 ml/well), incubated for 1 h, and then suspended in conditioned medium from ADSCs and plated in triplicate. The formation of tube-like structures was examined at 6 h. Quantitative analysis was conducted using ImageJ software (NIH, Bethesda, MD, USA). Tube formation was analyzed by quantifying the number of branches or tube length per high-powered field.

Statistical analysis

The results from at least three independent experiments are processed with GraphPad (San Diego, CA, USA) and are expressed as the mean ± standard deviation (SD). Statistical significance was evaluated by one-way analysis of variance (ANOVA) followed by Tukey's multiple comparison test or by Student's *t* test. A *P* value of less than 0.05 is considered statistically significant.

Results

Characterization of ADSCs and the responses of ADSCs to hypoxic stimulation

We first verified the stem cell properties of ADSCs. The cultured ADSCs were positive for CD29 and CD90, but were negative for CD34 and CD106 (Fig. 1a), and they could differentiate into adipocytes (Fig. 1b). First, we examined the secretion of a number of growth and inflammation factors that have been reported to be released from ADSCs. As the ELISA results showed, VEGFA was most significantly released during hypoxia treatment (Fig. 1c). Next, we exposed ADSCs to 1%, 3%, 10%, and 21% O_2 for 12 h, and then returned the cells to normoxia for 24 h. The protein levels of HIF1A and VEGFA could be remarkably induced by hypoxia in an oxygen concentration-dependent manner (Fig. 1d). The protein levels of HIF1A reached peak values at 1% O_2. Therefore, the following hypoxic exposure experiments were conducted under 1% O_2. As shown in Fig. 1e, the cell viability increased upon hypoxic stress. These data indicate that ADSCs grow faster upon hypoxic treatment; HIF1A and VEGFA might both be involved in ADSC cellular functions under hypoxic conditions.

Effects of ADSC paracrine on HDMEC functions upon hypoxia

Next, we investigated whether the increased VEGFA in ADSCs in hypoxic condition might contribute to the angiogenic ability of HDMECs. First, the suppressing efficiency

of si-VEGFA-1, si-VEGFA-2, and si-VEGFA-3 was determined using real-time PCR (Fig. 2a) and immunoblotting (Fig. 2b); si-VEGFA-1 was selected for use in further experiments.

Next, ADSCs were transfected with si-VEGFA and exposed to normoxia or hypoxia, and the conditioned media from the different groups were collected and used to incubate with HDMECs. As shown in Fig. 2c–e, the migration capacity, DNA synthesis ability, and tubule formation capacity of HDMECs in conditioned medium from hypoxia-stimulated ADSCs were significantly enhanced; however, these increases were significantly reversed by VEGFA silencing. These data indicate that VEGFA silencing in ADSCs attenuates the angiogenic capacity of HDMECs.

miR-590-3p targets the VEGFA 3′UTR to inhibit its expression

As we have mentioned, miR-153-3p, miR-590-3p, miR-26a-5p, miR-29b, miR-494, miR-16, and miR-320 are all angiogenesis-related miRNAs. Among these miRNAs, miR-590-3p was the only one that exhibited significantly

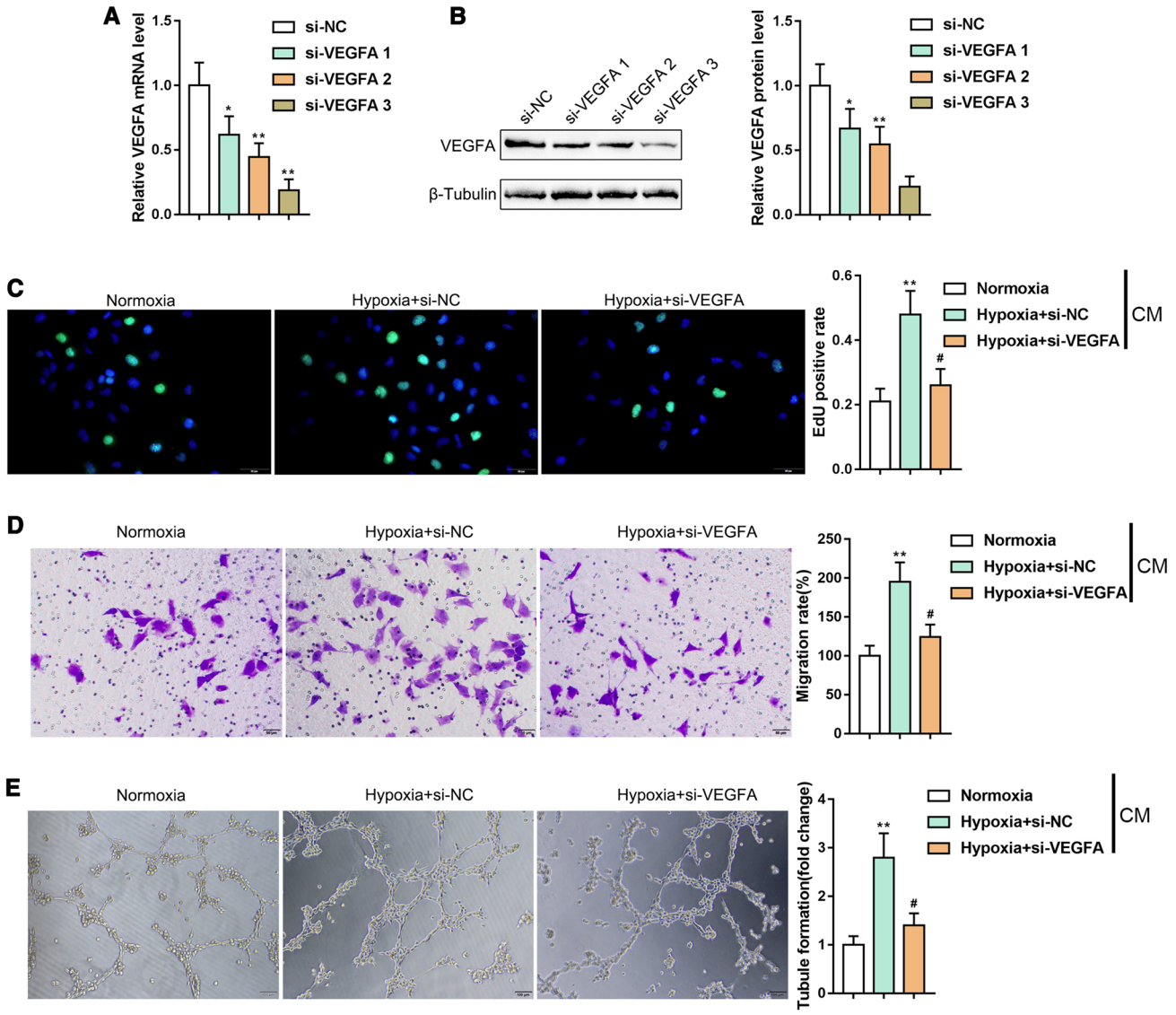

Fig. 2 Effects of ADSC paracrine on HDMEC functions upon hypoxia VEGFA silencing were obtained by transfection with si-VEGFA-1, si-VEGFA-2, and si-VEGFA-3, and the efficiency of reduced gene expression was measured by **a** real-time PCR ($n=5$) and **b** immunoblotting ($n=3$); si-VEGFA-1 was selected for further experiments. **c**–**e** ADSCs were transfected with si-VEGFA and then exposed to treatment with normoxia or hypoxia; HDMECs were cultured in the three different conditioned media and examined for DNA synthesis, migration and tubule formation capacity using EdU ($n=5$), Transwell ($n=5$), and tubule formation assays ($n=3$). $^{*}P<0.05$, $^{**}P<0.01$, compared to control group; $^{\#\#}P<0.01$, compared to hypoxia + si-NC (negative control) group. *CM* conditioned medium

downregulated expression in hypoxic conditions compared to that of cells in normoxia (Fig. 3a); thus, we hypothesize that miR-590-3p might participate in HDMEC angiogenesis in response to the paracrine effects of ADSCs. More importantly, as predicted by the lncTar online tool, miR-590-3p might suppress the expression of VEGFA via binding to its 3′UTR, indicating that miR-590-3p could be involved in HDMEC angiogenesis in a VEGFA-related manner.

To confirm the detailed involvement of miR-590-3p in VEGFA regulation, miR-590-3p mimic and anti-miR-590-3p were used to overexpress or inhibit miR-590-3p in ADSCs, respectively (Fig. 3b); VEGFA expression could be negatively modulated via miR-590-3p (Fig. 3c). To examine the putative binding between miR-590-3p and VEGFA, we conducted a luciferase reporter assay via the construction of wild- and mutant-type VEGFA 3′UTR luciferase reporter vectors that contain wild-type or mutated miR-590-3p binding sites (Fig. 3d). Figure 3e shows that the luciferase activity of the reporter vector with the wt-VEGFA 3′UTR was significantly reduced by miR-590-3p overexpression, whereas it was increased by miR-590-3p silencing. Mutating the predictive miR-590-3p binding site within the VEGFA 3′UTR abolished the alterations in luciferase activity (Fig. 3e). In summary, miR-590-3p inhibits VEGFA via direct targeting.

The involvement of miR-590-3p overexpression in VEGFA secretion and HDMECs

First, we confirmed the binding between miR-590-3p and VEGFA. Then we determined the specific cellular functions of miR-590-3p in regard to VEGFA and HDMEC angiogenesis. As shown in Fig. 4a, the hypoxia-induced increase in TGFβ1 secretion from ADSCs was significantly reduced by miR-590-3p overexpression. Figure 4b–d shows that hypoxia-induced HDMEC DNA synthesis ability, cell migration, and tubule formation could be significantly suppressed by miR-590-3p overexpression, indicating that miR-590-3p overexpression in ADSCs could suppress HDMEC angiogenesis by inhibiting the secretion of VEGFA in ADSCs.

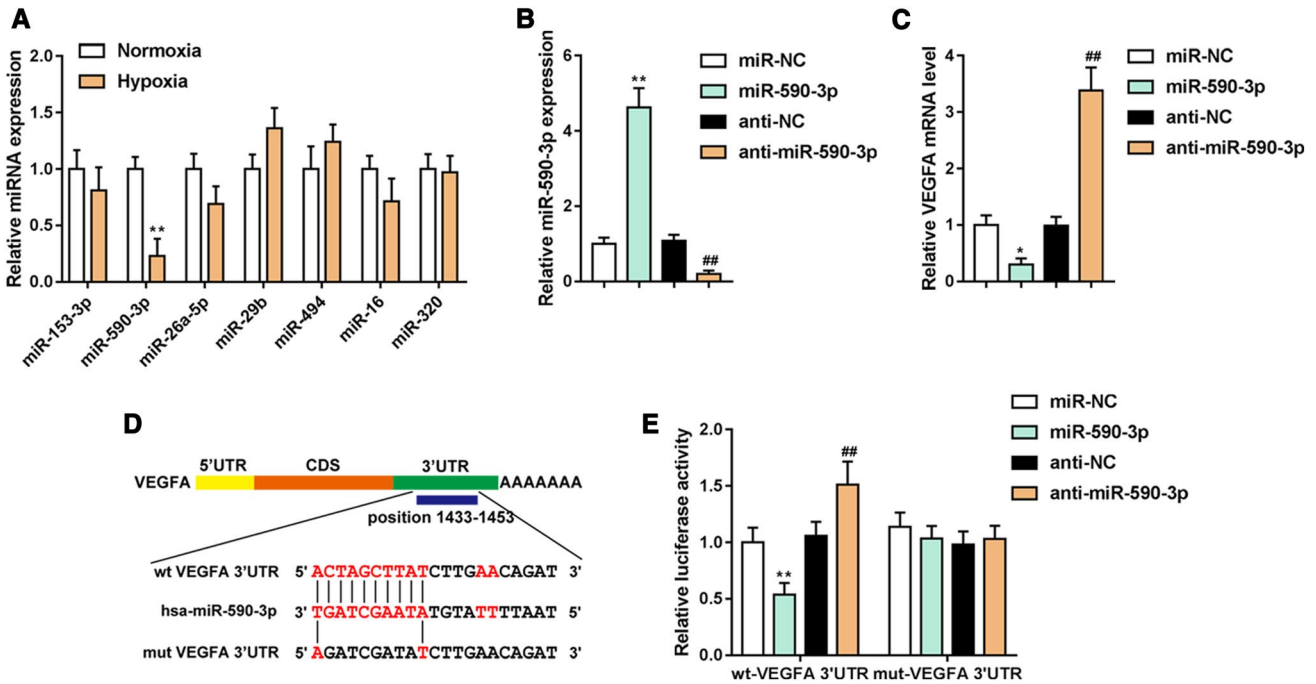

Fig. 3 miR-590-3p targets the 3′UTR of VEGFA to inhibit its expression. **a** ADSCs were exposed to 1% or 21% O_2 and examined for the expression of miR-153-3p, miR-590-3p, miR-26a-5p, miR-29b, miR-494, miR-16, and miR-320 by real-time PCR, $N=6$. **b** miR-590-3p expression was assessed in ADSCs following transfection with an miR-590-3p mimic or with anti-miR-590-3p, as confirmed by real-time PCR, $N=5$. **c** The expression of VEGFA in response to miR-590-3p overexpression or miR-590-3p inhibition was determined by real-time PCR, $N=5$. $^{*}P<0.05$, $^{**}P<0.01$, compared to the NC mimic group; $^{\#\#}P<0.01$, compared to the anti-NC group. **d** Wild-type and mutant-type VEGFA 3′UTR luciferase reporter vectors containing wild or mutated miR-590-3p binding were constructed. **e** 293T cells were cotransfected with these vectors and a miR-590-3p mimic or anti-miR-590-3p, and the luciferase activity was determined, $N=3$. $^{**}P<0.01$, compared to control group; $^{\#\#}P<0.01$, compared to miR-590-3p mimic group

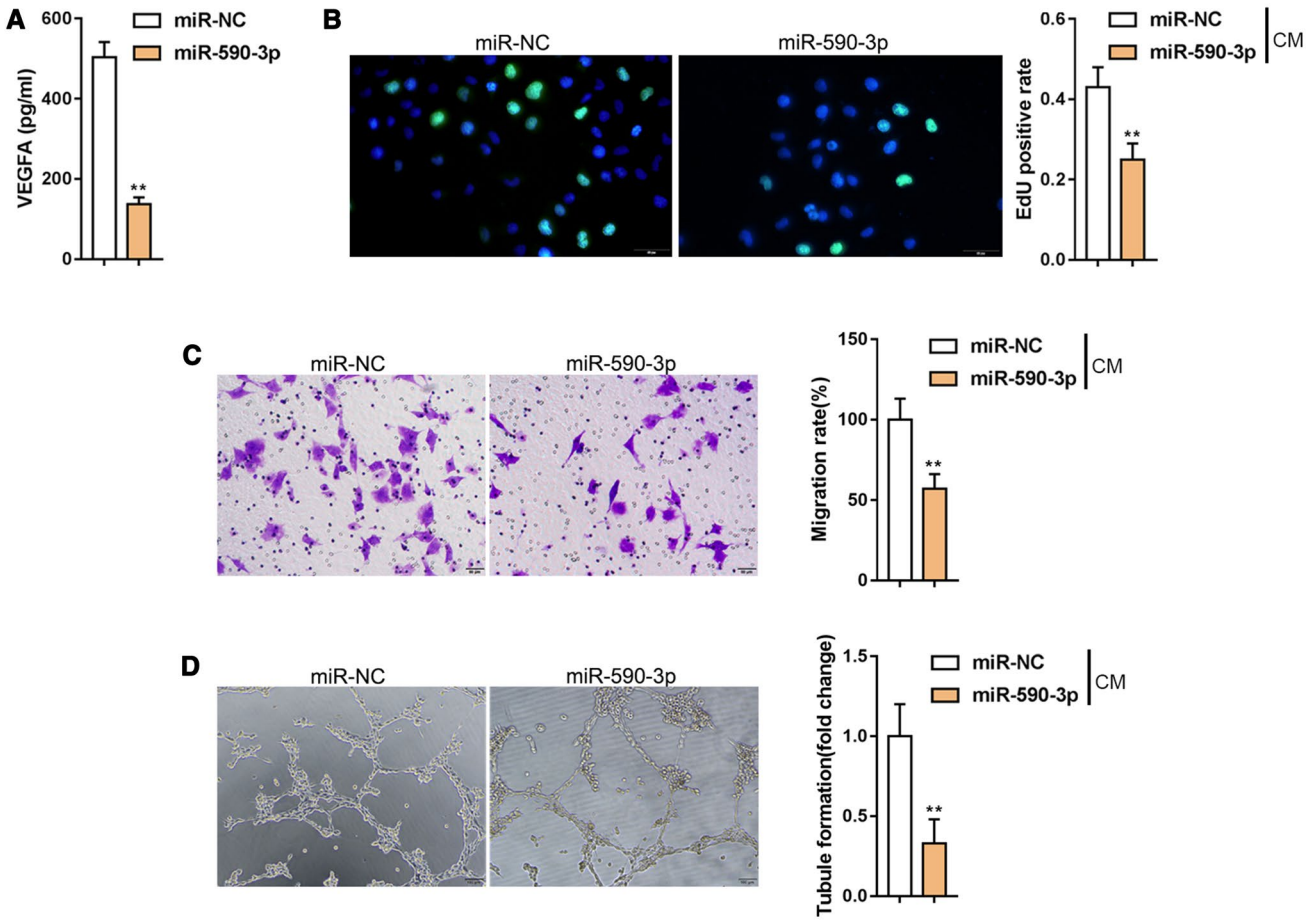

Fig. 4 Effect of miR-590-3p overexpression on VEGFA secretion and HDMECs. ADSCs were transfected with miR-590-3p mimic and exposed to 1% O_2 and examined for **a** VEGFA secretion ($n=3$); HDMECs were cultured with ADSCs conditioned medium and examined for **b** DNA synthesis ability, **c** cell migration, **d** tubule formation capacity by EdU ($n=5$), transwell ($n=5$), and tubule formation assays ($n=3$). $^{**}P<0.01$. *CM* conditioned medium

Dynamic effects of miR-590-3p and VEGFA upon HDMECs

Having demonstrated that miR-590-3p directly targets VEGFA, we next investigated whether the overexpression of VEGFA might reverse the effects of miR-590-3p overexpression in HDMEC angiogenesis. As shown in Fig. 5a, b, VEGFA mRNA expression levels and the VEGFA concentration within the culture medium were both remarkably suppressed by miR-590-3p overexpression, but they were enhanced by VEGFA overexpression; the effects of miR-590-3p overexpression could be significantly reversed by VEGFA overexpression.

Next, HDMECs were cultured in CMs from different ADSCs. The DNA synthesis, cell migration, and tubule formation of HDMECs could be significantly suppressed in miR-590-3p-overexpressing conditioned medium, but they could be enhanced in VEGFA-overexpressing conditioned medium; the effects of miR-590-3p overexpression were significantly reversed by VEGFA overexpression (Fig. 5c–e). These data indicate that miR-590-3p affects VEGFA secretion from ADSCs to modulate angiogenesis in HDMECs.

Discussion

Herein, we revealed that ADSC-secreted VEGFA served as a crucial growth factor involved in the paracrine-mediated ADSC modulation of HDMEC angiogenesis. HIF1A and VEGFA mRNA and protein expression could be markedly induced by hypoxia, and there was also an increase in ADSC cell viability. Incubation with conditioned medium from ADSCs treated with hypoxia significantly enhanced the angiogenesis capacity of HDMECs, while the conditioned medium from VEGFA-silenced ADSCs significantly reversed the angiogenesis capacity of HDMECs. Furthermore, miR-590-3p suppressed VEGFA expression

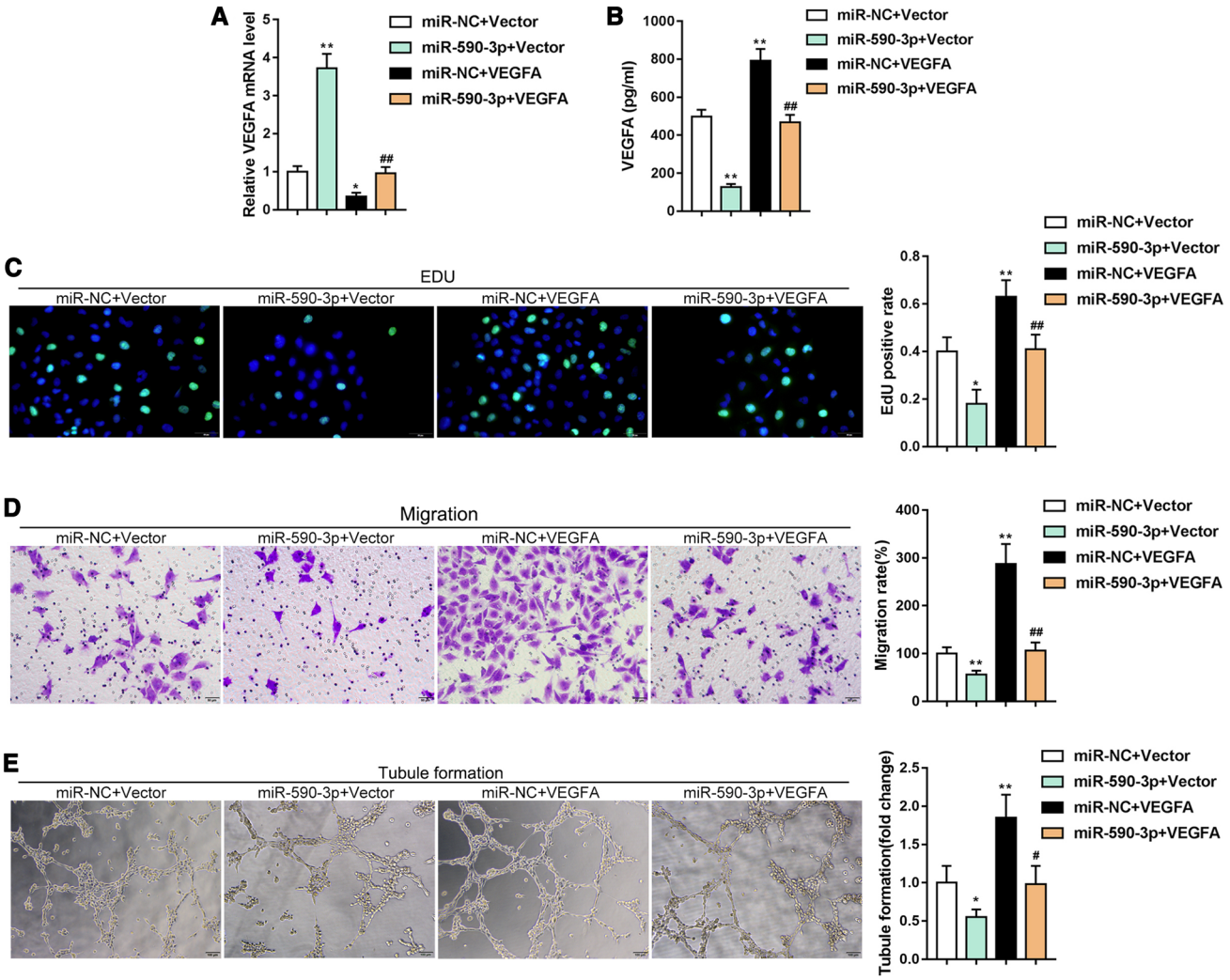

Fig. 5 Dynamic effects of miR-590-3p and VEGFA on HDMECs. ADSCs were co-transfected with miR-590-3p mimic and VEGFA-overexpressing vector upon 1% O_2 stimulation and examined for **a** VEGFA mRNA expression ($n=5$) and **b** VEGFA secretion ($n=3$); HDMECs were cultured with ADSCs conditioned medium and examined for **c** DNA synthesis ability, **d** cell migration, **e** tubule formation ability by EdU ($n=3$), transwell ($n=5$) and Tubule formation assays ($n=3$). $^{*}P<0.05$, $^{**}P<0.01$, compared to control group; $^{\#\#}P<0.01$, compared to NC mimic + VEGFA group. *CM* conditioned medium

and secretion through ADSCs via binding to its 3′UTR region, thereby modulating HDMEC angiogenesis by affecting the paracrine effects mediated by ADSCs; the involvement of miR-590-3p-overexpressed conditioned medium in HDMEC angiogenesis could be significantly reversed by VEGFA-overexpressed conditioned medium.

Hypoxia is one of the most critical characteristics of injured tissues. H1F1 has emerged as a crucial heterodimeric transcription factor, and the onset of its expression is considered one of the significant early cellular responses to low oxygen. Within hypoxic environments, HIF1 can target hypoxia-responsive elements (HREs) and induce the transcription of several target genes that contribute to angiogenesis [28]. Under hypoxic conditions, the transcription factor HIF-1 exerts a direct regulatory effect on the expression of VEGF [29, 30]. ADSCs have an excellent regenerative capacity, and multiple studies have proven that they augment tissue repairs by accelerating angiogenesis and fibrosis during the healing period [31–33]. The hypoxic conditions lead to excessive production of therapeutic paracrine factors by ADSCs, including VEGFA, thus repairing injured tissues [11]. During the C-reative protein-mediated proliferation and proangiogenic paracrine activity of ADSCs, HIF1α activation leads to the upregulation of VEGFA expression, which then significantly increases tubule formation [34]. In diabetic mellitus rat models, local intervention with ADSCs improves the neovascularization of diabetic ischemic skin by regulating the HIF-1α/VEGF pathway [35]. In the present study, hypoxia exposure induced significant increases in HIF1A and VEGFA mRNA and protein expression,

suggesting that VEGFA may be the critical factor in the paracrine factors from ADSCs in hypoxic conditions.

As a highly modulated process, angiogenesis results in the formation of new capillary sprouts from existing microvessel networks. During angiogenesis, new blood vessels form from original microvascular networks, migrate, proliferate and survive [36]. Several events may occur in the process of angiogenesis: the activation of endothelial cells and parental vasodilatation, the digestion of the basal membrane and the migration of endothelial cells from parental vessels to the sites where angiogenesis is necessary, which occurs via chemotaxis of monocytes, platelets, mast cells, and neutrophils [37]. It has been reported that the conditioned medium of ADSCs harvested under hypoxic conditions significantly promoted collagen synthesis and wound healing compared with what was observed in normoxic conditions [38]. To confirm the detailed involvement of ADSC-secreted VEGFA in endothelial cell angiogenesis, we incubated HDMECs with different CMs obtained from VEGFA-silenced or non-silenced ADSCs in hypoxic or normoxic conditions and found that hypoxia induces the secretion of VEGFA from ADSCs to promote HDMEC angiogenesis. After VEGFA silencing in ADSCs, the angiogenesis of HDMECs was also suppressed (Table 1).

In addition to growth factors, emerging evidence also indicates that miRNAs affect angiogenesis by modulating angiogenesis-associated cell proliferation, differentiation, apoptosis, migration, and tubule formation [39] by binding to downstream target mRNAs in their 3′UTRs to block translation or to induce degradation [40–43]. As we have mentioned, several miRNAs, including miR-153-3p, miR-590-3p, miR-26a-5p, miR-29b, miR-494, miR-16, and miR-320 can be essential for angiogenesis, depending on the cell type and their downstream targets. For example, miR-26a inhibits angiogenesis by targeting the HGF-VEGF axis in gastric carcinoma [44]. MiR-153 inhibits angiogenesis in HUVECs by targeting HIF1A [18]. Among the miRNAs mentioned above, miR-590-3p expression was remarkably suppressed by hypoxia in ADSCs. MiR-590-3p could bind to VEGFA. Similar to VEGFA-silenced conditioned medium, miR-590-3p-overexpressing conditioned medium significantly inhibited the angiogenesis of HDMECs, and VEGFA-overexpressing conditioned medium reversed the involvement of miR-590-3p overexpression in VEGFA secretion and HDMEC angiogenesis. In summary, miR-590-3p binds to VEGFA to inhibit VEGFA secretion from ADSCs, thereby inhibiting HDMEC angiogenesis. Zhou et al. also found that miR-590 inhibited angiogenesis by targeting the nuclear factor 90/VEGF axis in colorectal cancer [45].

In conclusion, the miR-590-3p/VEGFA axis modulates the paracrine secretion of VEGFA by ADSCs to affect the angiogenesis of HDMECs.

Acknowledgements This study was supported by the National Natural Science Foundation of China (General Program) (no. 81671964) and Natural Science Foundation of Hunan Province (2019JJ50847).

Compliance with ethical standards

Conflict of interest The authors declare that they have no conflict of interest.

References

1. Ucuzian AA, Gassman AA, East AT, Greisler HP. Molecular mediators of angiogenesis. J Burn Care Res. 2010;31:158–75.
2. Anderson JM, Rodriguez A, Chang DT. Foreign body reaction to biomaterials. Semin Immunol. 2008;20:86–100.
3. Zhao J, Yi C, Li L, et al. Observations on the survival and neovascularization of fat grafts interchanged between C57BL/6-gfp and C57BL/6 mice. Plast Reconstr Surg. 2012;130:398e–406e.
4. Pu LL. Mechanisms of fat graft survival. Ann Plast Surg. 2016;77(Suppl 1):S84–S8686.
5. Wang L, Wang F, Zhao L, Yang W, Wan X. Mesenchymal stem cells coated by the extracellular matrix promote wound healing in diabetic rats. Stem Cells Int. 2019;2019:9564869.
6. Gimble JM, Katz AJ, Bunnell BA. Adipose-derived stem cells for regenerative medicine. Circ Res. 2007;100:1249–60.
7. Suga H, Glotzbach JP, Sorkin M, Longaker MT, Gurtner GC. Paracrine mechanism of angiogenesis in adipose-derived stem cell transplantation. Ann Plast Surg. 2014;72:234–41.
8. Huang F, Zhu X, Hu XQ, et al. Mesenchymal stem cells modified with miR-126 release angiogenic factors and activate Notch ligand Delta-like-4, enhancing ischemic angiogenesis and cell survival. Int J Mol Med. 2013;31:484–92.
9. Zhu LP, Tian T, Wang JY, et al. Hypoxia-elicited mesenchymal stem cell-derived exosomes facilitates cardiac repair through miR-125b-mediated prevention of cell death in myocardial infarction. Theranostics. 2018;8:6163–77.
10. Tan Y, Nie W, Chen C, et al. Mesenchymal stem cells alleviate hypoxia-induced oxidative stress and enhance the pro-survival pathways in porcine islets. Exp Biol Med (Maywood, NJ). 2019;244:781–8.
11. Pankajakshan D, Agrawal DK. Mesenchymal stem cell paracrine factors in vascular repair and regeneration. J Biomed Technol Res. 2014;1:1.
12. Kinnaird T, Stabile E, Burnett MS, et al. Marrow-derived stromal cells express genes encoding a broad spectrum of arteriogenic cytokines and promote in vitro and in vivo arteriogenesis through paracrine mechanisms. Circ Res. 2004;94:678–85.
13. Kratchmarova I, Kalume DE, Blagoev B, et al. A proteomic approach for identification of secreted proteins during the differentiation of 3T3-L1 preadipocytes to adipocytes. Mol Cell Proteomics. 2002;1:213–22.
14. Rehman J, Traktuev D, Li J, et al. Secretion of angiogenic and antiapoptotic factors by human adipose stromal cells. Circulation. 2004;109:1292–8.
15. Han Y, Ren J, Bai Y, Pei X, Han Y. Exosomes from hypoxia-treated human adipose-derived mesenchymal stem cells enhance angiogenesis through VEGF/VEGF-R. Int J Biochem Cell Biol. 2019;109:59–68.
16. Yin KJ, Hamblin M, Chen YE. Angiogenesis-regulating microRNAs and ischemic stroke. Curr Vasc Pharmacol. 2015;13:352–65.

17. Thomou T, Mori MA, Dreyfuss JM, et al. Adipose-derived circulating miRNAs regulate gene expression in other tissues. Nature. 2017;542:450–5.
18. Li L, Wang M, Mei Z, et al. lncRNAs HIF1A-AS2 facilitates the up-regulation of HIF-1alpha by sponging to miR-153-3p, whereby promoting angiogenesis in HUVECs in hypoxia. Biomed Pharmacother. 2017;96:165–72.
19. Li TM, Liu SC, Huang YH, et al. YKL-40-induced inhibition of miR-590-3p promotes interleukin-18 expression and angiogenesis of endothelial progenitor cells. Int J Mol Sci. 2017;18:920.
20. Icli B, Wara AK, Moslehi J, et al. MicroRNA-26a regulates pathological and physiological angiogenesis by targeting BMP/SMAD1 signaling. Circ Res. 2013;113:1231–41.
21. Zhu ML, Yin YL, Ping S, et al. Berberine promotes ischemia-induced angiogenesis in mice heart via upregulation of microRNA-29b. Clin Exp Hypertens. 2017;39:672–9.
22. Esser JS, Saretzki E, Pankratz F, et al. Bone morphogenetic protein 4 regulates microRNAs miR-494 and miR-126-5p in control of endothelial cell function in angiogenesis. Thromb Haemost. 2017;117:734–49.
23. Lee JK, Park SR, Jung BK, et al. Exosomes derived from mesenchymal stem cells suppress angiogenesis by down-regulating VEGF expression in breast cancer cells. PLoS ONE. 2013;8:e84256.
24. Wang X, Huang W, Liu G, et al. Cardiomyocytes mediate anti-angiogenesis in type 2 diabetic rats through the exosomal transfer of miR-320 into endothelial cells. J Mol Cell Cardiol. 2014;74:139–50.
25. Bai X, Yan Y, Song YH, et al. Both cultured and freshly isolated adipose tissue-derived stem cells enhance cardiac function after acute myocardial infarction. Eur Heart J. 2010;31:489–501.
26. Liu Y, Wang Y, He X, et al. LncRNA TINCR/miR-31-5p/C/EBP-alpha feedback loop modulates the adipogenic differentiation process in human adipose tissue-derived mesenchymal stem cells. Stem Cell Res. 2018;32:35–42.
27. Liu ZB, Wang JA, Lv RQ. Downregulation of long non-coding RNA DBH-AS1 inhibits osteosarcoma progression by PI3K-AKT signaling pathways and indicates good prognosis. Eur Rev Med Pharmacol Sci. 2019;23:1418–27.
28. Kaur B, Khwaja FW, Severson EA, Matheny SL, Brat DJ, Van Meir EG. Hypoxia and the hypoxia-inducible-factor pathway in glioma growth and angiogenesis. Neuro Oncol. 2005;7:134–53.
29. Gao W, Qiao X, Ma S, Cui L. Adipose-derived stem cells accelerate neovascularization in ischaemic diabetic skin flap via expression of hypoxia-inducible factor-1alpha. J Cell Mol Med. 2011;15:2575–85.
30. Forsythe JA, Jiang BH, Iyer NV, et al. Activation of vascular endothelial growth factor gene transcription by hypoxia-inducible factor 1. Mol Cell Biol. 1996;16:4604–13.
31. Komiyama S, Sakakura C, Murayama Y, et al. Adipose-derived stem cells enhance tissue regeneration of gastrotomy closure. J Surg Res. 2013;185:945–52.
32. Kaisang L, Siyu W, Lijun F, Daoyan P, Xian CJ, Jie S. Adipose-derived stem cells seeded in Pluronic F-127 hydrogel promotes diabetic wound healing. J Surg Res. 2017;217:63–74.
33. Wu YY, Jiao YP, Xiao LL, et al. Experimental study on effects of adipose-derived stem cell-seeded silk fibroin chitosan film on wound healing of a diabetic rat model. Ann Plast Surg. 2018;80:572–80.
34. Chen J, Gu Z, Wu M, et al. C-reactive protein can upregulate VEGF expression to promote ADSC-induced angiogenesis by activating HIF-1alpha via CD64/PI3k/Akt and MAPK/ERK signaling pathways. Stem Cell Res Ther. 2016;7:114.
35. Yu WY, Sun W, Yu DJ, Zhao TL, Wu LJ, Zhuang HR. Adipose-derived stem cells improve neovascularization in ischemic flaps in diabetic mellitus through HIF-1alpha/VEGF pathway. Eur Rev Med Pharmacol Sci. 2018;22:10–6.
36. Griffioen AW, Molema G. Angiogenesis: potentials for pharmacologic intervention in the treatment of cancer, cardiovascular diseases, and chronic inflammation. Pharmacol Rev. 2000;52:237–68.
37. Hillen F, Griffioen AW. Tumour vascularization: sprouting angiogenesis and beyond. Cancer Metastasis Rev. 2007;26:489–502.
38. Lee EY, Xia Y, Kim WS, et al. Hypoxia-enhanced wound-healing function of adipose-derived stem cells: increase in stem cell proliferation and up-regulation of VEGF and bFGF. Wound Repair Regen. 2010;17:540–7.
39. Sun LL, Li WD, Lei FR, Li XQ. The regulatory role of microRNAs in angiogenesis-related diseases. J Cell Mol Med. 2018;22:4568–87.
40. Thamotharan S, Chu A, Kempf K, et al. Differential microRNA expression in human placentas of term intra-uterine growth restriction that regulates target genes mediating angiogenesis and amino acid transport. PLoS ONE. 2017;12:e0176493.
41. Lucas T, Schafer F, Muller P, Eming SA, Heckel A, Dimmeler S. Light-inducible antimiR-92a as a therapeutic strategy to promote skin repair in healing-impaired diabetic mice. Nat Commun. 2017;8:15162.
42. Siomi H, Siomi MC. Posttranscriptional regulation of microRNA biogenesis in animals. Mol Cell. 2010;38:323–32.
43. Karreth FA, Tay Y, Perna D, et al. In vivo identification of tumor-suppressive PTEN ceRNAs in an oncogenic BRAF-induced mouse model of melanoma. Cell. 2011;147:382–95.
44. Si Y, Zhang H, Ning T, et al. miR-26a/b inhibit tumor growth and angiogenesis by targeting the HGF-VEGF axis in gastric carcinoma. Cell Physiol Biochem. 2017;42:1670–83.
45. Zhou Q, Zhu Y, Wei X, et al. MiR-590-5p inhibits colorectal cancer angiogenesis and metastasis by regulating nuclear factor 90/vascular endothelial growth factor A axis. Cell Death Dis. 2016;7:e2413.
46. Kim U, Shin DG, Park JS, et al. Homing of adipose-derived stem cells to radiofrequency catheter ablated canine atrium and differentiation into cardiomyocyte-like cells. Int J Cardiol. 2011;146:371–8.